PHYSICAL REVIEW D
PARTICLES AND FIELDS

THIRD SERIES, VOLUME 52, NUMBER 11 — 1 DECEMBER 1995

ARTICLES

Relative abundance of ^{3}He and ^{4}He in cosmic rays near 10 GV

Y. Hatano, Y. Fukada, and T. Saito
Institute for Cosmic Ray Research, University of Tokyo, Tanashi, Tokyo

H. Oda
Department of Physics, Kobe University, Kobe, Japan

T. Yanagita
Gunma College of Technology, Maebashi, Japan
(Received 20 April 1993; revised manuscript received 21 June 1995)

The abundance ratio of ^{3}He and ^{4}He has been measured at six different atmospheric depths, from 8 g/cm^2 to 23 g/cm^2, employing the geomagnetic method. The ratio at the top of the atmosphere was obtained by fitting the observed six ratios. The observed ratio is consistent with the standard propagation model of cosmic rays.

PACS number(s): 98.70.Sa, 96.40.De

It is known from observed ratios of secondary to primary cosmic rays (e.g., [Li+Be+B]/[C+O] and sub Fe/Fe) that cosmic rays of several GeV/nucleons traverse about 6–8 g/cm^2; this path decreases with increasing energy. This rigidity-dependent confinement of cosmic rays in the Galaxy led to the standard propagation model of cosmic rays. The ratios ^{3}He/^{4}He and ^{1}H/^{2}H have also been used to study the propagation of cosmic rays. On the other hand, the ratio ^{3}He/^{4}He at 6 GeV/nucleon as measured by Jordan and Meyer [1] gave a path length of 15 g/cm^2, greater than that predicted by the standard propagation model. The abundance of cosmic-ray antiprotons at GeV energies [2] has been shown to be a factor 3–4 greater than that of secondary antiprotons based on the standard propagation model. An excess in the positron flux has also been reported at high energies [3]. If these results are correct, the origin or the propagation mechanism of primary H and He might differ from those of cosmic ray nuclei with $Z \geq 6$.

We carried out measurements on the ratio ^{3}He/^{4}He at six different depths in the atmosphere by using the geomagnetic field as a rigidity filter [4].

In measurements of cosmic-ray rare components by balloon borne instruments, the secondary particles produced by nuclear collisions with the atmospheric nuclei above the instrument are a serious source of background [6] because of the uncertainty in the fragmentation probabilities. This effect to our measurement will be discussed afterward.

Figure 1 shows a schematic diagram of the instrument used for these measurements. It consists of two scintillation counters $S1$ and $S2$ used to define the incident charge, two scintillation counters $P1$ and $P2$, for determining the particles position, and a high-pressure gas Cherenkov counter for measuring the particle velocity. The scintillators $S1$ and $S2$ are 70 cm in diameter and 1 cm thick. Each of them is housed in an octagonal shaped light diffusion box and is viewed by eight 5 in. photomultiplier tubes (PMT's, Hamamatsu R877), which are divided into two groups of four PMT's to provide two independent measurements of the scintillation light. Each of the two scintillators $P1$ and $P2$ (70 cm in diameter and 1.5 cm thick) is housed in an octagonal box; PMT's are placed on the four sides of the box. The shape, dimen-

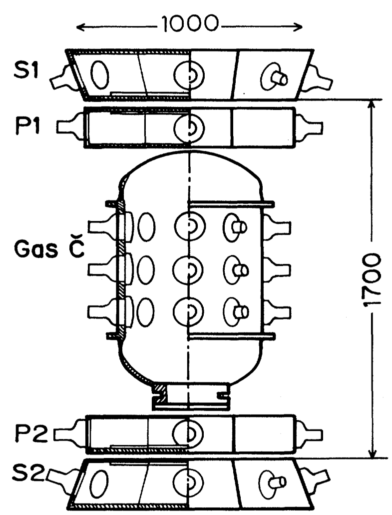

FIG. 1. Schematic cross section of the instrument.

sions, and refractivity of the inside wall of the $P1$ and $P2$ boxes are optimized in order to get strong nonuniformity in the light collection, leading to better position resolution. The position resolution is 2 cm around the edge and 5 cm at the center of the scintillators.

In order to get a refractive index $n = 1.0179$ corresponding to a threshold energy of 4.1 GeV/nucleon (equivalent to the effective cutoff rigidity of our experimental site, 9.8 GV for ^{4}He) two kinds of gas, CF_4 (index of refraction $n = 1.0006$ at 1 atm. and 20 °C) and $CClF_3$ ($n = 1.000\,783$ at 1 atm and 20 °C) were mixed at a pressure of 30 atmosphere (CF_4:$CClF_3$=35:65). The effective refractive index of the mixed gas was measured by π^- accelerator beams of momentum 0.3–5 GeV/c at KEK-PS. The pure CF_4 gas produces the scintillation light. The scintillation light from the CF_4 gas is quenched and then decreased by adding the $CClF_3$. No scintillation light (less than 1% of the Cherenkov light) was observed with the chosen gas mixture. The gas is enclosed in a cylindrical aluminum container of 60 cm in diameter and 110 cm height. The inside wall of the container was coated with reflective paint. In the commercially available $BaSO_4$ paint, acrylic emulsion is generally used as a binder producing Cherenkov light. In order to avoid this background, we used a homemade $BaSO_4$ paint, without acrylic binder. The Cherenkov light was collected by 24 5-in. PMTs (Hamamatsu R877) divided into three groups of eight PMT's to provide three independent measurements. The instrument was calibrated with cosmic-ray muons at the ground level. The total collected light for the gas Cherenkov counter amounted to 60 photoelectrons for relativistic cosmic-ray muon.

The geometric factor of the instrument defined by $S1$ and $S2$ is 474 cm^2 sr, and the total weight is 490 kg. The instrument was flown from the Sanriku Balloon Center of the ISAS on September 16, 1989. The balloon was floating within a region of vertical cutoff rigidity 9.5–10.1 GV. About 4 million events were collected in 36 h at six different altitudes (8.5 ± 0.3, 9.5 ± 0.4, 10.8 ± 0.4, 13.4 ± 0.7, 15.9 ± 0.9, and 22.7 ± 0.8 g/cm^2). The incident direction of the particles to the geomagnetic field line was measured by two right angle magnetometers. The gain drift of the detectors was corrected by monitoring the peak channel of the proton pulse height distribution.

In the two-dimensional histograms (scatter plots) of two pulse heights from the same counter, the events outside 3 standard deviations (3σ) from the average response of cosmic rays were rejected *a priori*, in such a way avoiding the background due to counter noise and particles hitting the PMT's. The position counter unfortunately broke during the balloon flight and the particle trajectory could not be measured for about 50% of the data. As the full opening angle of our trigger counters, $S1$ and $S2$, is 22 °, the maximum difference of particle track lengths in the counter is 8%; this adds to the uncertainty in charge measurement as $\Delta Z/Z = 0.04$. The charge resolution was 0.1 unit of charge for He without the track length measurement. All the data were used together irrespective of rigidity. To avoid the mass dependence in detecting He nuclei, which is originated from the difference of collision mean free paths between ^{3}He and ^{4}He, only He nuclei identified with the top scintillator $S1$ were accepted for the analysis. In fact, the $S1$ counter is placed below 0.5 g/cm^2, to be compared to 12.5 g/cm^2 above $S2$.

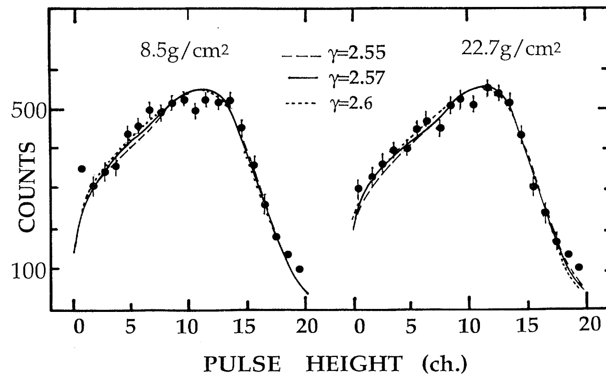

FIG. 2. The pulse height distributions of the Cherenkov counter at the depths of 8.5 and 22.7 g/cm^2. The solid curve shows the best fit to the data with $\gamma = 2.57$, the dashed and dotted curves are for $\gamma = 2.55$ and 2.60, respectively.

Examples of the observed pulse height distribution of the Cherenkov counter are shown in Fig. 2 for two different measurements at 8.5 and 22.7 g/cm^2. The solid curve in Fig. 2 shows the best fit with $\gamma = 2.57$, while the dashed and dotted curves show those with $\gamma = 2.55$ and 2.59, respectively, where γ is the index of the ^{4}He rigidity spectrum. The fitting process will be discussed afterward.

The pulse height distribution of the gas Cherenkov counter is a function of four parameters, the ratio ^{3}He/^{4}He, the cutoff rigidity R_c at the experimental site, the index γ of the He rigidity spectrum, and the standard deviation σ(He). The standard deviation is given by $\sigma(\mathrm{he})^2 = \sigma_{\mathrm{ph}}^2 + \sigma^2$, where σ_{ph} is the statistical error in the photoelectron number determined by ground level muon. The δ-ray effects and other experimental uncertainties are included in one parameter σ determined by fitting the observed pulse height distribution. The rela-

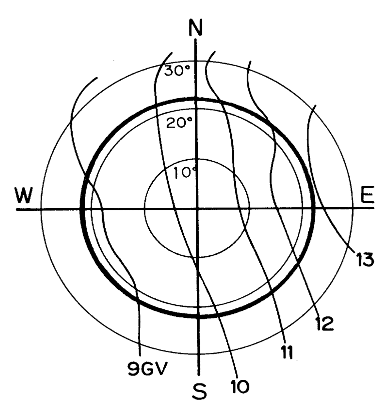

FIG. 3. Contour map of rigidity at Sanriku. The solid circle shows the rigidity region covered by the instrument.

tion between the cutoff rigidity and the particle zenithal and azimuthal angles of incidence was calculated at a given altitude of balloon flight by using the trajectory tracing method. The solid circle in Fig. 3 shows the rigidity region covered by our instrument at Sanriku. The effective cutoff rigidity was calculated to be 9.8 GV by taking into account our instrumental configuration. In the trajectory tracing, particles can sometimes enter a region with rigidity smaller than the cutoff one, but they never appear where the rigidity is less than 8 GV.

The pulse height distributions of Cherenkov counter, which are normalized to the peak value of the distribution are shown in Fig. 4. The dashed curves show the expected ^{3}He pulse height distribution. The calculation of these distributions included the effect of the fuzziness of opening angles. In the figure, the bold arrows indicate the threshold energies for ^{4}He(4.1 GeV/nucleon) and ^{3}He(5.7 GeV/nucleon), corresponding to the cutoff $R_c = 9.8$ GV. As shown in Fig. 4, the ratio of ^{3}He/^{4}He affects only the pulse height distribution below the channel near the peak (indicted by an asterisk), that is, the distribution above this channel depends on the index γ of the ^{4}He spectrum and on the σ value, but it is not sensitive to the ^{3}He/^{4}He ratio. To simplify the decoupling procedure, two of the three parameters (γ and σ) were determined at first by

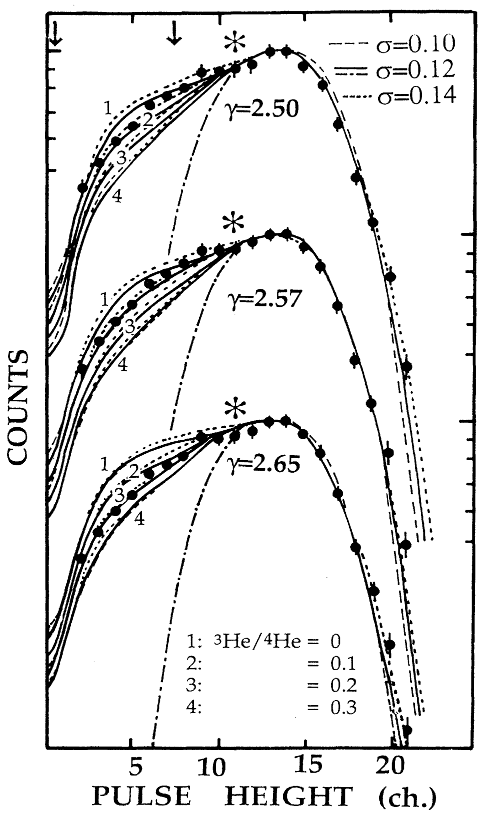

FIG. 4. The calculated pulse height distribution of Cherenkov counter with the three parameters of the ^{3}He/^{4}He ratio, σ and γ. Each curve is normalized to the peak value. The bold arrows indicate the threshold of ^{4}He and ^{3}He at a cutoff rigidity of 9.8 GV. The dashed curve shows the distribution for ^{3}He. The data point are of 9.5 g/cm^2.

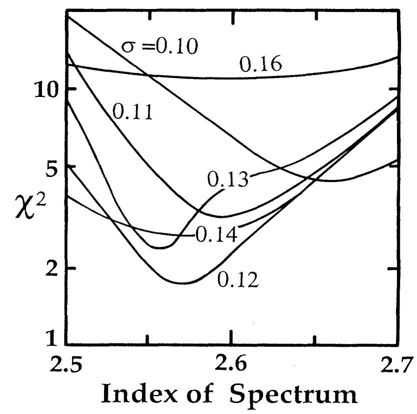

FIG. 5. The χ^2 fit (degrees of freedom = 10) for determining an exponent γ of ^{4}He rigidity spectrum and σ.

fitting the data in the region above the marked channel. An example of the χ^2 fit results is shown in Fig. 5. In each of the six independent measurements, we found a minimum value $\chi^2 \sim 2.6$ for γ, and ~ 0.12 for σ. Values of $\gamma = (2.57 \pm 0.05)$ and $\sigma = (0.12 \pm 0.02)$ were obtained by this χ^2 fit. The published data about the rigidity spectral index of ^{4}He range from $\gamma = (2.47 \pm 0.05)$ [10] to $\gamma = (2.71 \pm 0.05)$ [11,5]. Our measurements were made near the solar maximum period. Taking into account the effect of solar modulation, the derived spectrum index is consistent with those measurements. As indicated by Webber *et al.* [5], the derived ratio ^{3}He/^{4}He depends strongly on the chosen value of γ. Thus, it is mostly important to measure the rigidity spectrum in the isotopic composition study using the geomagnetic field. Using the three parameters, R_c, γ, and σ so obtained, the ratio ^{3}He/^{4}He was then determined by the χ^2 fit of the pulse height distributions below the asterisk marked channel at each altitude.

Figure 6 shows the dependence of the observed ratio ^{3}He/^{4}He on the atmospheric depth. The errors in this figure include statistical errors as well as uncertainties

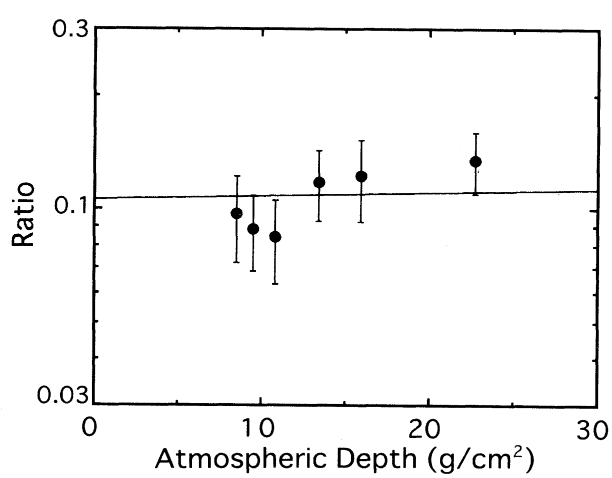

FIG. 6. The observed ratios ^{3}He/^{4}He at six different atmospheric depths. The errors include the error caused by the uncertainty of the γ.

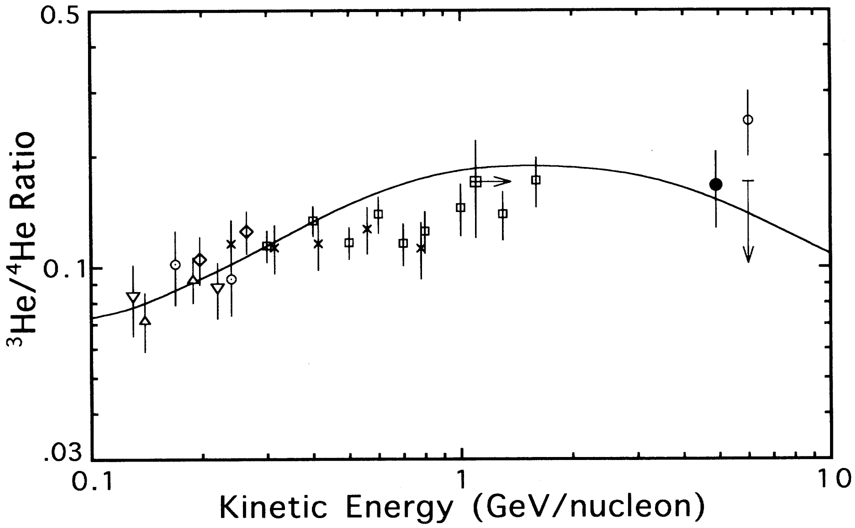

FIG. 7. Observed ^{3}He/^{4}He ratios. The present result is shown at the mean energy by the solid circle. The open circle shows that by Jordan *et al.* [1]. The downward arrow shows the reexamination of the work of Jordan by Webber *et al.* [5], adopting the different index of spectrum which was used by the original authors. The rectangles show that by Ficenec *et al.* [8], crosses by Webber *et al.* [9]. The other data were quoted from Mewaldt [6]. Solid curve is a prediction from the standard propagation model [6].

in γ and σ. The velocity distribution of ^{3}He and ^{4}He is already decided by the geomagnetic field before these particles enter into the atmosphere. Even if a ^{4}He interacts with the overlying atmosphere above the counter and converts to ^{3}He, which has mostly same kinetic energy as the parent ^{4}He, observed Cherenkov distribution does not change.

The ratio $R(x) = {}^3\text{He}/{}^4\text{He}$ at an atmospheric depth x is described by the formula

$$R(x) = R(0)\,\exp(-x/\Lambda_3)/\{\exp(-x/\Lambda_4) + P_{43}(\Lambda/\lambda_4)[\exp(-x/\Lambda_4) - \exp(-x/\Lambda_3)]\}\ ,$$

where $R(0)$ is the ^{3}He/^{4}He ratio at the top of the atmosphere, P_{43} is the fragmentation probability of producing ^{3}He from ^{4}He, λ_4 is the inelastic interaction mean free path of ^{4}He in the atmosphere, and $\Lambda_4 = \lambda_4/(1 - P_{44})$, $\Lambda_3 = \lambda_3/(1 - P_{33})$. We used the same value for P_{33} and P_{44} ($= 0.05 \pm 0.03$, most commonly used), because these values are not sensitive to the derived ^{3}He/^{4}He ratios. The value of the second term of the denominators is corresponding to the produced ^{3}He and smaller than that of the first term, then we can rewrite the formula as

$$R(x) \approx R(0)\,\exp(-x/\Lambda_3)/\exp(-x/\Lambda_4)\ .$$

The ratio $R(0) = (0.106 \pm 0.025)$ was obtained by the χ^2 fit to the data. The solid line in Fig. 6 shows the best-fit curve.

The ratio R_r at 9.8 GV can be converted to the ratio at the equivalent kinetic energy of 4.9 GeV/nucleon by the formula

$$R_e = R_r (R/P_n)^{\gamma_3-\gamma_4} (2/A_4)^{1-\gamma_4}/(2/A_3)^{1-\gamma_3}\ ,$$

where R_e is the ratio at a given kinetic energy; R_r is the ratio at the rigidity R; P_n is the momentum per nucleon; γ_3, γ_4, A_3, and A_4 are the spectral index and mass for ^{3}He and ^{4}He, respectively.

When we use the same $\gamma = 2.57$ for ^{3}He and ^{4}He spectrum, we find $R = (0.167 \pm 0.04)$. For secondary cosmic rays such as ^{3}He, we have to choose an index γ higher than that of primary nuclei. However, this factor is slightly different (5.5%) but does not affect the conclusion. The ratio at energy at 4.9 GeV/nucleon is shown in Fig. 7 together with those from other measurements [7]. The solid curve depicts the dependence of this ratio on kinetic energies as calculated by Mewaldt [6] based on the standard propagation model. Our result does not show any excess of ^{3}He and is consistent with the standard propagation model.

The authors wish to express their thanks to Professor T. Hara and K. Yamamoto for their assistance through the experiment, and to Professor R. N. Boyd, Ohio State University for his critical reading of the manuscript. We are indebted to the staffs of the Sanriku Balloon Center for their successful balloon flight and staffs of the KEK PS. for their kind support to the calibration work. This work was partly supported by the ISAS grant for instrumental development.

[1] Steven P. Jordan and Peter Meyer, Phys. Rev. Lett. **53**, 505 (1984); Steven P. Jordan, Astrophys. J. **291**, 207 (1985); R. Dwyer, S Jordan, and P. Meyer, Nucl. Instrum. Methods **224**, 247 (1984).
[2] R. L. Golden *et al.*, Phys. Rev. Lett. **43**, 1196 (1979); E. A. Bogomlov *et al.*, in *Proceedings of the 16th International Cosmic Ray Conference*, Kyoto, Japan, 1979 (Institute for Cosmic Ray Research, Tokyo, 1979), Vol. 1, p. 330; A. Buffington *et al.*, Astrophys. J. **248**, 1179 (1981).
[3] A. Buffington, C. D. Orth, and G. F. Smoot, Astrophys. J. **199**, 699 (1975); D. Muller and J. Tang, *ibid.* **312**, 183 (1987).
[4] B. Peters, Nucl. Instrum. Methods **121**, 205 (1974).
[5] W. R. Webber, R. L. Golden, and R. A. Mewaldt, Astrophys. J. **312**, 178 (1987).
[6] R. A. Mewaldt, Astrophys. J. **311**, 979 (1986).
[7] R. A. Mewaldt, in *Cosmic Abundances of Matter*, edited by C. Jake Waddington, AIP Conf. Proc. No. 183 (AIP, New York, 1989), p. 124.
[8] D. J. Ficenec *et al.*, in *Cosmic Ray Conference*, Proceedings of the 23rd International Conference, Calgary, Canada, 1993, edited by R. B. Hicks *et al.* (World Scientific, Singapore, 1994), Vol. 1, p. 515.
[9] W. R. Webber *et al.*, Astrophys. J. **380**, 230 (1991).
[10] L. H. Smith *et al.*, Astrophys. J. **180**, 987 (1973).
[11] R. L. Golden *et al.*, in *Proceedings of the 19th International Cosmic Ray Conference*, La Jolla, California, 1985, edited by F. C. Jones *et al.*, NASA Conf. Publ. 2376 (Goddard Space Flight Center, Greenbelt, MD, 1985), Vol. 2, p. 1.